MOTORBIKE MODELING AND CONTROL

Joao Sequeira[1] and Marco di Vittori [1]
[1]*Instituto Superior Tecnico, Technical University of Lisbon, Portugal*
joao.silva.sequeira@ist.utl.pt, marco@frenk.com

Keywords: Kinematics, Dynamics, PID control, MPC control, Nonlinear control

Abstract: This paper surveys the kinematics of bikes and details the construction of a dynamics model for a motorbike using the Lagrangian approach. Using data from a typical sports motorbike, a dynamics model is obtained by symbolic computation. This model, of high algebraic complexity, is then wrapped as a function and used for control purposes. Control strategies based on PID, MPC, and nonlinear control are discussed and simulation results for each of them are presented.

1 INTRODUCTION

The study of bicycle modeling and control dates back to the last years of 19th century, namely through the work of F.J. Whipple (see for instance (Limebeer and Sharp, 2006)). In recent times there has been a renewed interest in this type of vehicles from an academic viewpoint and extreme riding, as in racing,is still challenging, namely in what concerns the development of control strategies for autonomous or quasi-autonomous motion.

Related work in literature is extensive. Surveys on a wide range of bicycle models are presented in (Aström et al., 2005), (Limebeer and Sharp, 2006). A linearized model for an uncontrolled bicycle was presented in (Schwab et al., 2004) with multiple simplifications, namely the bike is formed by rigid bodies, the wheels have no width, and the rider position is constant.

Realistic motorcycle dynamics have an algebraically complexity higher than those of simple bycicles. Among the relevant work, the geometry of the contact between tyres and the road, the tyre shear force and moment descriptions, as functions of load, slip and camber, the tyre relaxation properties, rear suspension, rider behavior, and steering control have been addressed in (Sharp et al., 2004). Only PID based strategies were considered for speed and steering control, though with adjustable gains.

Some aspects related to the steering angle control in human driving are addressed in (Popov et al., 2010). The stability dependency on control parameters is analyzed from the human automatisms processes when riding a motorbike, including a precognitive component related to the rider's experience, a compensatory component as the closed loop control, and a pursuit component as a feedforward term to handle throttle and braking. Optimal, Model Predictive (MPC), and PID based steering control are claimed to match the three stage control used by human riders.

This paper surveys kinematics models for bycicles and their extensions to commercial motorbikes in section 2. The dynamics model is derived in section 3, using the classic constrained Lagrangian method. This model is then used in section 4 to test trajectory tracking using PID, MPC, and nonlinear laws. Simulation results are compared with a reference trajectory obtained from telemetry data from a real motorbike in a racetrack. Section 5 discusses the results obtained with the models based uniquely on the kinematics and those obtained using dynamics models.

2 KINEMATICS

Using the simplified geometry in figure 1 the kinematics equations for a simple motorbike model are simply, (Limebeer and Sharp, 2006),

$$\dot{x} = v\cos(\psi) \tag{1}$$

$$\dot{y} = v\sin(\psi) \tag{1a}$$

$$\dot{\psi} = \frac{v\tan(\delta)}{w\cos(\varphi)} \tag{1b}$$

where w is the wheelbase, assumed constant.

The rake angle, γ (see figure 2) can be easily included and (1b) becomes,

$$\dot{\psi} = \frac{v\tan(\delta\cos(\gamma))}{w\cos(\varphi)} \tag{2}$$

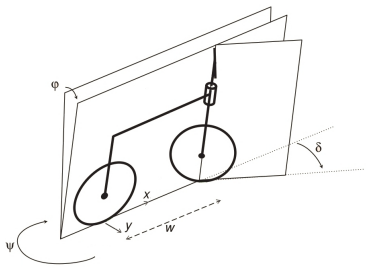

Figure 1: Simplified bike geometry (adapted from (Limebeer and Sharp, 2006)).

A typical rake in resting conditions value for a commercially available motorbike is $\gamma = 23.5°$. This model assumes no front or rear suspensions which in reality induce variations in w.

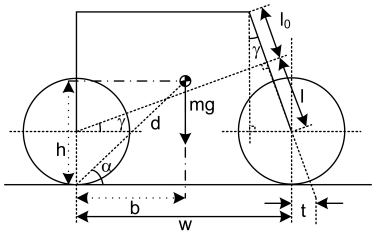

Figure 2: Front fork, rake angle, and trail distance.

The front fork length is given by $l = w\ \sin(\gamma)$ (see figure 2). Assuming that the chassis is rigid $w\ \cos(\gamma)$ must be constant

It is straightforward to obtain the following relation,

$$w = \frac{l}{\sqrt{w_0^2 \cos^2(\gamma_0) + l^2}} \tag{3}$$

where w_0 and γ_0 represent the wheelbase distance and rake angle in resting conditions. Substituting in (2) the kinematics model including the front fork length l is,

$$\dot{\psi} = \frac{v \tan\left(\delta \frac{|w_0 \cos(\gamma_0)|}{\sqrt{w_0^2 \cos^2(\gamma_0) + l^2}}\right)}{\frac{l^2}{\sqrt{w_0^2 \cos^2(\gamma_0) + l^2}} \cos(\varphi)} \tag{4}$$

A typical value for the front fork trail is around 119.0 mm.

In most of the current motorbikes the rear wheel is connected to the chassis through a moving swingarm. The typical geometry used by manufacturers introduces a new variable, β, representing the angle between the swingarm and the horizontal x axis (figure 3). The length of the swingarm is denoted by s.
The corresponding model can be obtained by replacing the variables w_0 and γ_0 in (4) by $w_0 - (s - \cos(\beta - \gamma_0))$ and $l + \sin(\beta - \gamma_0)$ respectively.

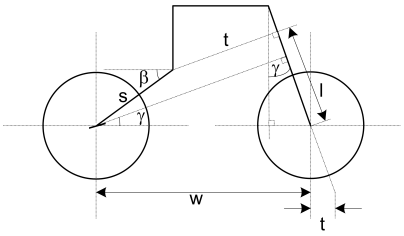

Figure 3: Swingarm connecting the back wheel to the bike frame.

$$\dot{\psi} = \frac{v \tan\left(\delta \frac{|(w_0 - (s - \cos(\beta - \gamma_0)))\cos(\gamma_0)|}{\sqrt{(w_0 - (s - \cos(\beta - \gamma_0)))^2 \cos^2(\gamma_0) + (l + \sin(\beta - \gamma_0))^2}}\right)}{\frac{(l + \sin(\beta - \gamma_0))^2}{\sqrt{(w_0 - (s - \cos(\beta - \gamma_0)))^2 \cos^2(\gamma_0) + (l + \sin(\beta - \gamma_0))^2}} \cos(\varphi)} \tag{5}$$

Model (5) accounts for most of the geometric aspects in current motorbike designs. Even though the instantiation done with typical values for some of the parameters, the model shows the complex structure of a motorbike kinematics.

From (1) and (2), if w increases then $\dot{\psi}$ decreases. This may be a desirable feature in conditions where ψ is subject to disturbances. For example, under hard braking conditions any disturbances in δ and v will be affected by the gain $1/w$. If this gain decreases then also will the effects of these disturbances in ψ.

A similar reasoning can be made when the front fork is considered and this suggests an alternative kinematics, namely using and additional swingarm at the front of the motorbike, instead of the common front fork. In terms of the model previously developed there is no γ angle and an additional variable β_2 is introduced to represent the angle of the front swingarm.

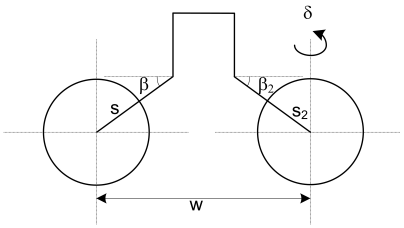

Figure 4: Double swingarm geometry.

As before, using typical values from commercially available motorbikes yields or the rotation (w now depends on both the front and rear swingarm position),

$$\begin{aligned} w &= s\cos(\beta) + s_2\cos(\beta_2) + 231 \\ \dot{\psi} &= \frac{v\,\delta}{578.5(\cos(\beta) + \cos(\beta_2) + 231)\cos(\varphi)} \end{aligned} \tag{6}$$

where β and β_2 values will be in the range $[0.4^\circ, 13.4^\circ]$.

Double swingarm kinematics has been seldom used in production bikes (the reader can check the Yamaha GTS 1000 and Bimota Tesi). Even in racing applications, which in a sense tend to use more extreme designs, there is a single known case, the Elf 500cc motorbike, which raced during the 80's decade. This type of kinematics is sometimes referred as being extremely stable under hard braking conditions.

Combinations of the fork and swingarm in the front geometry are currently being used (see for instance the telelever and duolever systems used by BMW). As aforementioned, the idea is to increase the wheelbase under braking to improve the rideability.

3 DYNAMICS

Computing the dynamics of a constrained multibody vehicle, as a motorbike, is relatively straightforward assuming that the motorbike is composed by multiple rigid bodies with known geometry and mass distribution properties. However, it is seldom the case that perfect information is available. An extreme example is the sloshing effect caused by the fuel moving freely in the tank (in some bikes the fuel can account for 6% of the total mass). Therefore, simplified models of mass distribution are often assumed.

The strategy followed in this paper is to compute a symbolic model, using the Lagrangian technique. The resulting model is then wrapped as a Matlab function that can be used as a blackbox model for experimenting purposes. This model accounts for the main kinetic energy sources in a motorbike, namely, the engine, and wheels and bike main body under leaning and turning (the terms due to the motion of the swingarm and front fork are not considered). Potential energy is also not considered in this model as the variations involved when the bike leans or moves along height variations tend to be small and do not disturb the structure of the model.

The total kinetic energy including terms due to leaning and turning, linear velocity, front and rear wheels, and engine is thus given by,

$$K = \frac{m(\dot{\varphi}h + \dot{\psi}b)^2}{2} + \frac{mR_r^2\dot{\theta}_m^2 g_r^2}{2} + \\ + \frac{m_f R_r^2 \dot{\theta}_m^2 g_r^2}{4\cos^2(\delta\cos(\gamma))} + \frac{m_r r_r^2 \dot{\theta}_m^2 g_r^2}{4} + \frac{m_m r_m^2 \dot{\theta}_m^2}{4} \quad (7)$$

where b, h are the mass center coordinates (see Figure 2, note that the total mass of the frame, suspensions, and non-rotating parts of the engine, m, are concentrated at a single point). The front and back wheels have masses m_f and m_r, respectively, and m_m is the engine's rotating mass and inertias modeled as thin disks. The wheel radius are r_f and r_r, respectively for the front and back wheels, whereas r_m is the radius of the engine's rotating mass. The angular velocity of the engine is $\dot{\theta}_m$ leading to angular velocities for the forward and back wheels of $\dot{\theta}_f = \frac{\dot{\theta}_m g_r R_r}{\cos(\delta)R_f}$ and $\dot{\theta}_r = g_r\dot{\theta}_m$, respectively. The ratio between the engine and rear wheel angular velocities is denoted g_r and R_r is the rear wheel effective radius which accounts for the leaning of the bike as $R_r = r_t\cos(\varphi) + r_w\sqrt{1-(r_r/r_w\sin(\varphi))^2}$ and r_w is the wheel rhym radius, r_t is the tyre tube radius and $r_r = r_w + r_t$.

Table 1 lists the main physical parameters and values used in the model.

$\alpha = 0.698rad$	$d = 0.85m$	$m = 180Kg$
$m_f = 3.3Kg$	$m_r = 4.5Kg$	$m_m = 2.5Kg$
$r_r = 0.3149m$	$r_m = 0.1m$	$g_r = 0.192$
$r_w = 0.2277m$	$\lambda_0 = 23.5^\circ$	

Table 1: Dynamics parameters (after a commercial motorbike).

The theory for constrained Lagrangian systems is well understood when the constraints are holonomic or semi-holonomic. See for instance (Chessé and Bessonet, 2001; Campion et al., 1996; McClamroch and Wang, 1988) for structures with holonomic constraints and (Flannery, 2005) for nonholonomic ones.

The ideal 2-wheel motorbike has two classes of constraints, (i) the contact with the ground which constrains the vertical movement, and (ii) the car-like non-holonomic constraint, $v = \dot{\psi}r_1$ (which is also commonly written as $\dot{x}\sin\psi - \dot{y}\cos\psi = 0$), that inhibits side-slipping (r_1 represents the curve radius) and the rolling constraint $v = \cos(\psi)\dot{x} + \sin(\psi)\dot{y}$, that inhibits forward-skidding. In a real motorbike the variety of situations rends difficult an accurate identification of the constraints. For example, the geometry of the contact between the tyres and the ground imposes that there is indeed a small amount of slide-slippage and hence the non side-slipping constraint is only valid under unrealistic conditions.

A common strategy when identifying constrained dynamics is to rely on a priori knowledge on the physical effects affecting the robots (see for instance (Aström et al., 2005; Yi et al., 2009)). The constraining torques are thus simplified and are considered the direct consequence of the reaction forces applied on the center of mass and formed by the gravitational and centrifugal forces that constrain the motorbike at the contact points between the wheels and

the ground. These forces are calculated as $N = mg$ and $T = mR_r g_r \dot{\theta}\dot{\psi}$, respectively as the vertical force due to gravity depending on the total mass, m, and gravity g and the centrifugal force due to $\dot{\psi}$ turning speed. These forces are related to φ as the torque $\Gamma_{\varphi ext} = Nh\sin(\varphi) - Th\cos(\varphi)$ so the total model has the following structure.

$$M \begin{bmatrix} \ddot{\varphi} \\ \ddot{\theta} \end{bmatrix} + V = \begin{bmatrix} \Gamma_\varphi \\ \Gamma_\theta \end{bmatrix} + \begin{bmatrix} Nh\sin\varphi - Th\cos\varphi \\ 0 \end{bmatrix} \tag{8}$$

with M and V as determined by the free Lagrangian computed from (7), and Γ_φ, Γ_θ being functions respectively of the steering angle δ and the force F_f exherted on the footpegs by the driver.

4 CONTROL

The dynamics model (8) was first controlled by a PID controller. Figure 5 shows the results obtained for a section of the Montmelo racetrack near Barcelona, Spain. This section of the racetrack includes fast and slow portions where different control parameters are required. Thus, a supervisor controller changes the PID gains at appropriate times, when the bike switches between the different sections of the track.

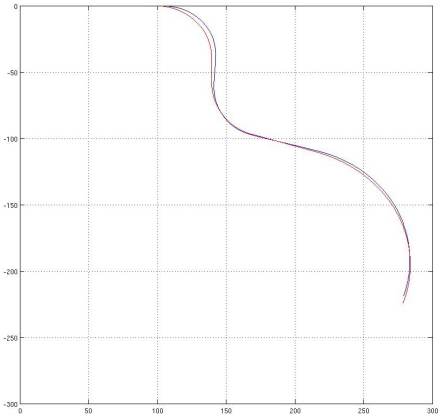

Figure 5: PID based control.

A natural alternative approach, widely used in the literature (see for instance (Rau and Schröder, 2002)) is the Model Predictive Control (MPC). Roughly, the MPC computes the open loop controls during a finite horizon that minimize at each instant k a cost $J(k) = \sum_{i=1}^{N_y} w_i \left(r(k+i) - y(k+i)\right)^2 + w_u \sum_{i=1}^{N_u} u(k+i)^2$, where r is a reference, y the output and u the controls of the system, and uses the first controls in the optimal sequence. At subsequent steps the procedure is repeated, thus closing the control loop.

Figure 6 shows the MPC applied to the kinematic models described in previous section, (1) to (6). A discrete range of controls is used, namely $\delta \in \{-1, -0.5, -0.2, 0, 0.2, 0.5, 1\}$. Linear velocity is assumed constant, $v = 1$, and wheelbase $w_0 = 1.3$m. Control horizon $N = 3$ $N_y = N_u = 3$ and control weights are $w_u = 10$ and $w_i = 2 \times 10^{-4}$ for the simpler models and $w_y = 10^{-8}$ for model (5). Only the first control of the sequence computed at each instant is used, that is, a new control is computed at each time step.

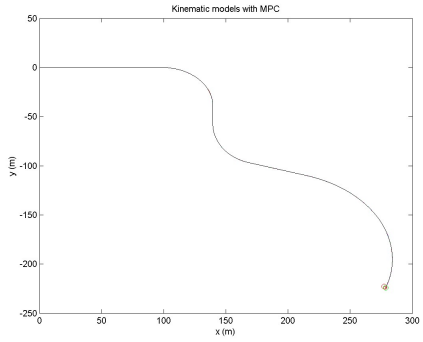

(a) Complete trajectory

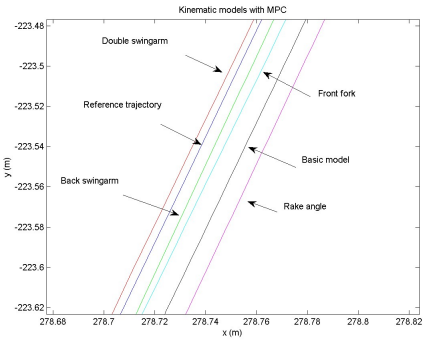

(b) Trajectory detail

Figure 6: Kinematic models with MPC.

Even though the trajectories are shown for fixed values of the parameters $\lambda_0, l, \beta, \beta_2$, the curves suggest that the double swingarm and front fork models may be preferable in a real racing scenario, where the small differences shown may be very relevant.

Figure 7 illustrates the MPC results when the full dynamics model is used with $w_u = 10$ and $w_i = 10^{-4}$. PID control was used to drive the leaning to 0 and an engine torque bounded at 0.8 Nm.

The nonlinear law used to control steering is common in Robotics (and known to stabilize linearized unicycle models) and is of the form,

$$\delta = -K_1 v\, l + K_2 |v| \left(\psi_{ref} - \psi\right) \tag{9}$$

where l is the signed distance defined by the projection of the position of the motorbike onto the refer-

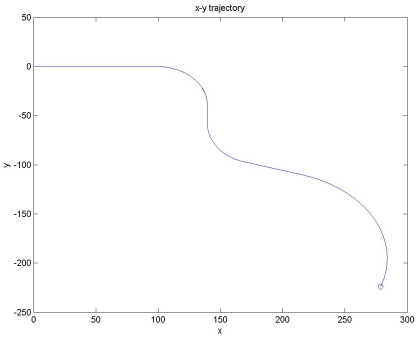

(a) Trajectory

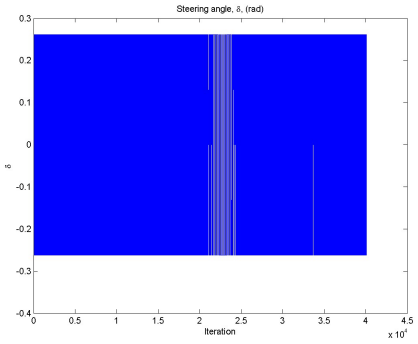

(b) Steering angle

Figure 7: Dynamics model and MPC.

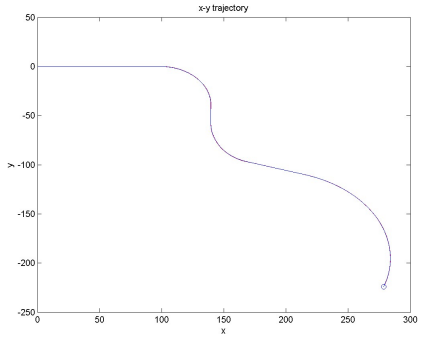

(a) Trajectory

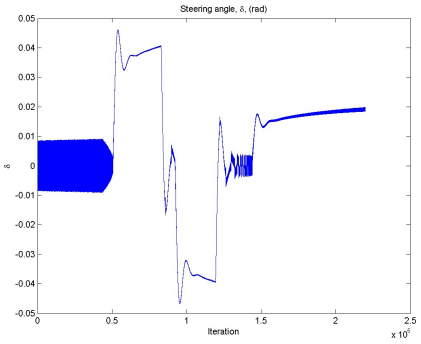

(b) Steering angle

Figure 8: Nonlinear control law with $K_1 = 5$, $K_2 = 10$.

ence path, v is the linear velocity, ψ, ψ_{ref} are the orientation of the bike and the corresponding reference, and K_1, K_2 tuning constants. Leaning was controlled using a PID.

Figure 8 illustrates the performance of the motorbike when the steering is controlled by (9) (see appendix 6 for a stability proof).

The jerk in both controls is significantly smaller than with MPC control and the leaning angle error is also smaller.

5 CONCLUSIONS

Starting from basic models for bicycles, the paper introduces a number of kinematics features that are common in motorbikes. These features are shown to influence the kinematic models significantly and hence justify the use of complex models to describe bikes in the context of real applications. MPC control was shown to yield small differences among the models that nonetheless may be relevant in extreme riding conditions such as racing.

A dynamics model, accounting for the bike and engine motion, is presented and controlled using PID, MPC, and a nonlinear law. As with the kinematic models, the three techniques show very small differences in the trajectory following error, though presenting very different computational requirements.

Even though the simplifying assumptions taken, i.e., on point masses, inertias, rigidity of the different bodies, driver model reduced to the footpeg force input, the algebraic complexity of the free Lagrangian is high. This justifies the use of a further simplifying strategy, that is, the inclusion of constraint forces directly in the model. The different control strategies provide interesting results, with the nonlinear law exhibiting a far more reasonable behavior from a practical application perspective, with less jerk, and suggest that the whole model can be used to further proceed the research on the full racing problem. Future work also involves the testing of a supervisory control layer to optimize the selection of parameters for the leaning and velocity loops.

ACKNOWLEDGEMENTS

This work was partially supported by FCT project PEst-OE/EEI/LA0009/2011.

REFERENCES

Abdallah, C., Dawson, D., Dorato, P., and Jamshidi, M. (1990). Survey of Robust Control for Rigid Robots. In *Procs. American Control Conf.*

Anderson, R. (1989). Passive Computed Torque Algorithms for Robots. In *Procs. 28th Conf. on Decision and Control*.

Aström, K., Klein, R., and Lennartsson, A. (2005). Bicycle Dynamics and Control. *IEEE Control Systems Magazine*.

Campion, G., Bastin, G., and D'Andrea-Novel, B. (1996). Structural Properties and Classification of Kinematic and Dynamic Models of Wheeled Mobile Robots. *IEEE Trans. on Robotics and Automation*, 12(1).

Chessé, S. and Bessonet, G. (2001). Optimal dynamics of constrained multibody systems. Application to bipedal walking synthesis. In *Procs of the IEEE Int. Conf. on Robotics and Automation*. Seoul, Korea, May 21-26.

Flannery, M. (2005). The enigma of nonholonomic constraints. *American Journal of Physics*, 73(3):265–272.

Limebeer, D. and Sharp, R. (2006). Bicycles, Motorcycles, and Models. *IEEE Control System Magazine*.

McClamroch, N. and Wang, D. (1988). Feedback Stabilization and Tracking of Constrained Robots. *IEEE Transactions on Automatic Control*, 33(5):419–426.

Ortega, R., Loría, A., Nicklasson, P., and Sira-Ramírez, H. (1998). *Passivity-based Control of Euler-Lagrange Systems*. Springer.

Ortega, R. and Spong, M. (1988). Adaptive motion control of rigid robots: A tutorial. In *Procs. IEEE Conf. Decision and Control*.

Popov, A., Rowell, S., and Meijaard, J. (2010). A review on motorcycle and rider modeling for steering control. *Vehicle System Dynamics*, 48(6):775–792.

Rau, M. and Schröder, D. (2002). Model Predictive Control with Nonlinear State Space Models. In *Procs. of the American Control Conference (AMC 2002)*.

Schwab, A., Meijard, J., and Papadopoulus, J. (2004). Benchmark results on the linearized equations of motion of an uncontrolled bicycle. In *Proc. 2nd Asian Conf. Multibody Dynamics*.

Sharp, R., Evangelou, S., and Limebeer, D. (2004). Advances in the Modeling of Motorcycle Dynamics. *Multibody System Dynamics*, (12):251–283.

Yi, J., Zhang, Y., and Song, D. (2009). Autonomous Motorcycles for Agile Maneuvers, Part I: Dynamics Modeling. In *Procs. Joint 48th IEEE Conf. on Decision and Control and 28th Chinese Control Conf.*

Yu, H. and Antsaklis, P. (2009). Passivity-Based Distributed Control of Networked Euler-Lagrange Systems With Nonholonomic Constraints. Technical report. Technical Report of the ISIS Group at the Univ. of Notre Dame, ISIS-09-003.

6 Nonlinear Controller Stability

The dynamics (8) can be written in more general terms as,

$$M(\varphi,\theta)\begin{bmatrix}\ddot{\varphi}\\ \ddot{\theta}\end{bmatrix}+V(\varphi,\dot{\varphi},\theta,\dot{\theta})= \tag{10}$$

$$=\begin{bmatrix}2.148F_f\\ T_m\end{bmatrix}+\begin{bmatrix}Nh\sin(\varphi)-Th\cos(\varphi)\\ 0\end{bmatrix}$$

$$\dot{\psi}=0.046\tan(\delta\cos(\gamma))\,\dot{\theta}/\cos(\varphi) \tag{10b}$$

Unconstrained Lagrangian systems can be shown to have the passivity property, (Ortega and Spong, 1988) even when subject to external forces/torques, such as the case of a motorbike, (Yu and Antsaklis, 2009). Also, a feedback control of a passive system with a passive controller yields a stable system (see (Abdallah et al., 1990)) and even in the case of contact forces and uncertainties in M a PD-like structure was shown to be able to stabilize the system (see (Anderson, 1989)).

Therefore, it remains to be shown here that (i) decoupling the control for F_f, T_m, δ does not disturb the passivity property, and (ii) the nonlinear law (9) also drives the tracking error to zero.

The passivity property is closed under the addition operation on controls. In what concerns control inputs F_f, T_m, decoupling the control law means that each control input is driven by an independent controller. In the experiments, T_m was chosen as a pulse of constant height 0.1 Nm, going to zero as $\dot{\theta}_m > 0.8$ rad/s and hence it verifies the passivity property. As for F_f, it was generated after a PID, meaning that it also verifies the passivity property (see (Ortega et al., 1998)). It is enough to described the control as $[\Gamma_\varphi, \Gamma_\theta] = [\Gamma_\varphi, 0] + [0, \Gamma_\theta]$ to verify that the decoupling of the controls preserves the passivity property of the overall system.

As for the control input δ, substituting the control law (9) in (10b) yields an equation of the form,

$$\dot{e}_\psi = -\tan\left((-K_1\, v\, l + K_2|v|e_\psi)\cos(\gamma)\right)K \tag{11}$$

where the orientation error is $e_\psi = \psi_{ref} - \psi$, and $K = 0.046\,\dot{\theta}/\cos(\varphi)$ is nonzero for the relevant ranges of the argument, i.e., $v \in (0, +\infty)$ and $\varphi \in (-pi/2, \pi/2)$.

The fixed point of (11) is thus obtained either when $v = 0$, or when $l = 0$ and $\psi = \psi_{ref}$, and hence the nonlinear control law is able to make the motorbike track the reference trajectory.